2010-09

Erbium and ytterbium codoped titanoniobophosphate glasses for ion-exchange-based planar waveguides

Journal of the American Ceramic Society,Malden : Wiley-Blackwell Publishing,v. 93, n. 9, p. 2689-2692, Sept. 2010
http://www.producao.usp.br/handle/BDPI/49918

journal

J. Am. Ceram. Soc., 93 [9] 2689–2692 (2010)
DOI: 10.1111/j.1551-2916.2010.03768.x

Erbium and Ytterbium Codoped Titanoniobophosphate Glasses for Ion-Exchange-Based Planar Waveguides

José Carlos Bozelli,[‡] Luiz Antonio de Oliveira Nunes,[§] Fernando Aparecido Sigoli,[‡] and Italo Odone Mazali[†,‡]

[‡]Institute of Chemistry, University of Campinas–UNICAMP, Campinas, SP, 13083–970 Brazil

[§]Institute of Physics, University of São Paulo–USP, São Carlos, SP, 13660–970 Brazil

This work presents the optical properties of erbium-doped and erbium/ytterbium codoped Na_2O–Al_2O_3–TiO_2–Nb_2O_5–P_2O_5 glass systems and also the characterization of planar waveguides obtained by typical thermally assisted $Ag^+ \leftrightarrow Na^+$ ion-exchange process. The glass systems allow the preparation of single mode and multimode planar waveguides presenting a strong and relatively broad emission at 1536 nm. The emission signal in the infrared region is intensified for silver-containing samples when compared with free-silver samples. The emission signal intensification may be attributed to a nonplasmonic energy transfer from silver species to Er^{3+} ions as no bands related to surface plasmon resonance (SPR) of silver nanoparticles were observed.

I. Introduction

Phosphate glasses, with additional network-forming oxides and one or more network-modifying oxides, have chemical durability comparable with silicate glasses.[1–3] The optical properties of phosphate glasses show many favorable features for use in optical devices because of their excellent transparency and good mechanical and thermal stability.[4] The phosphate matrix exhibits a high ability to dissolve considerable amounts of alkaline, alkaline earth, transition metal, and also rare-earth ions.[5] Sodium containing phosphate glasses suitable for ion-exchange processes are getting a lot of interest for the preparation of optical planar and channel waveguides. In this context, rare-earth-doped waveguides have been prepared by the $Ag^+ \leftrightarrow Na^+$ thermal assisted ion exchange method using Er^{3+} and Yb^{3+} co-doped phosphate glass, attracting great attention in the field of optoelectronic devices.[6–14] The preparation of waveguides by the thermally assisted $Ag^+ \leftrightarrow Na^+$ ion-exchange method is a well-established process because the cations have a similar radius ($Na^+ = 98$ pm and $Ag^+ = 113$ pm)[15] and because the Na^+ ions also exchange well with Ag^+ ions for waveguide preparation.[7] Moreover, Ag^+ ions present incomplete $(n-1)d$ shells being more polarizable than Na^+ ions. The polarization of the Ag^+ ions increases the refractive index that can be tailored using concentration gradients in order to obtain planar or channel waveguides with high or low refractive index variation. The thermally assisted $Ag^+ \leftrightarrow Na^+$ ion-exchange process nowadays is attracting renewed interest for its simplicity, flexibility, and low fabrication cost. Additionally, it is possible to accurately control the refractive index variation of the waveguide by changing the Ag^+ concentration in the melting bath and the glass composition.[16–18]

Phosphate glasses are being used as promising materials applied to photonic devices, such as erbium-doped waveguide amplifiers (EDWA), because they are able to dissolve considerable amounts of active ions that are required to prepare channel waveguide amplifiers.[7–13] In the case of EDWA, a large amount of Er^{3+} ions is required due to its small absorption cross section at the excitation region of telecommunication interest and also due to the short length of channel waveguides. Further, the use of considerable amounts of active ions, sensitizing ions such as Yb^{3+}, may also be required in order to enhance the absorption cross-section at 980 nm and improve the Er^{3+} ion emission at 1530 nm by nonradiative energy transfer from the sensitizer to the active ions. On the other hand, the emission intensity of rare-earth ions may be improved by a local electrical field enhancement around them.[19] The enhancement of the electrical field may be achieved by metal surface collective electronic oscillation, known as SPR of noble metal nanoparticles, such as silver or gold, present in dielectric matrices.[19] Recently, a nonplasmonic mechanism for enhancing the electrical field around rare-earth ions has been described in the literature as a nonradiative energy transfer from defects, related to the presence of noble metal species, such as dimers and trimers to rare-earth ions.[20] The nonplasmonic energy transfer mechanism may significantly enhance the rare-earth emission by two orders of magnitude even under nonresonant rare-earth excitation in the UV-Vis region.[21]

Recently, our group has reported the synthesis of a new phosphate glass system–Na_2O–Al_2O_3–TiO_2–Nb_2O_5–P_2O_5 (NAPTN)-with a high resistance against chemical attack, exhibiting dissolution rates $< 1.8 \times 10^{-9}$ $g \cdot (cm^2 \cdot min)^{-1}$, in 1.0 mol/L aqueous HCl solution at 298 K.[3] In silicate glasses, Al_2O_3 is typically used to improve the solubility and homogeneity and to reduce the formation rate of rare-earth ion pairs and clusters.[22] In phosphate glasses, Al_2O_3 promotes the same role as those verified for silicate glasses and also acts as an ionic cross-linker between different chains, inhibiting hydration reactions, and giving outstanding chemical durability to phosphate glasses. Nb_2O_5 and TiO_2 are normally added to increase the linear refractive index and chemical durability of phosphate glass, Nb_2O_5 being more effective than TiO_2 for improving the linear refractive index and chemical durability.[3]

In the present work, we present the optical properties of erbium-doped and erbium/ytterbium-codoped Na_2O–Al_2O_3–TiO_2–Nb_2O_5–P_2O_5 glass systems and also the characterization of planar waveguides obtained by typical thermally assisted $Ag^+ \leftrightarrow Na^+$ ion-exchange process, which may be comparable with well-established phosphate-based materials used in the state-of-art of active optical devices.

II. Experimental Procedure

(1) Glass Preparation

Glasses having compositions of $20Na_2O$–$(5-x-y)Al_2O_3$–xEr_2O_3–yYb_2O_3–$30Nb_2O_5$–$15TiO_2$–$30P_2O_5$ (mol%), were prepared by a conventional melt-quenching method.[3] The compositions of

J. Heo—contributing editor

Manuscript No. 27180. Received 30 November 2009; approved 4 March 2010.
This work was financially supported by FAPESP, CNPq, and CAPES.
[†]Author to whom correspondence should be addressed. e-mail: mazali@iqm.unicamp.br

Table I. Nominal Glass System Compositions

	$20Na_2O–(5–x–y)Al_2O_3–xEr_2O_3–yYb_2O_3–30Nb_2O_5–15TiO_2–30P_2O_5$		
Sample	$(5–x–y)Al_2O_3$	xEr_2O_3	yYb_2O_3
NAPTN	5	0	0
NAPTN:Er	4	1	0
NAPTN:Er:Yb	2	1	2

the glasses are summarized in Table I. The raw materials used were reagent-grade Na_2CO_3 (Merck, São Paulo, Brazil), Al_2O_3 (Baker, Phillipsburg, NJ), P_2O_5 (Merck), anatase-TiO_2 (Baker), and Nb_2O_5 (CBMM—Companhia Brasileira de Metalurgia e Mineração, Araxá, Brazil). Stoichiometric compositions of batch materials were melted under air at 1673 K for 3 h in platinum crucibles that were placed in an electric furnace (EDG, São Carlos, Brazil). The mixtures were stirred several times during the melting process in order to obtain homogeneous melts. At the end of the refining process, the temperature was decreased to 1473 K and the melts were poured onto carbon plates, annealed at (T_g −40 K) for 16 h, and cooled slowly to release the thermal stress associated with these glasses during the quenching process. For each NAPTN glass system, two monoliths were prepared from different melts and each monolith was diced into 2-mm-thick disks and polished for use for characterization and also for the ion-exchange process.

(2) Ion-Exchange Process

Planar waveguides were prepared by typical thermally assisted $Ag^+ \leftrightarrow Na^+$ ion-exchange processes. In summary, a mixture of 97.33 g $NaNO_3$ (Synth, São Paulo, Brazil) and 2.67 g $AgNO_3$ (Aldrich, São Paulo, Brazil) was melted at 673 K in a quartz tube of a vertical tubular furnace (BP Engenharia, Campinas, Brazil). The NAPTN disks were inserted in the melt and kept immersed for 1 h. The surface-modified glasses, identified hereafter as NAPTN:Ag; NAPTN:Er:Ag; NAPTN:Er:Yb:Ag, were withdrawn from the furnace and subsequently washed several times using distilled water.

(3) Characterization

Absorption spectra (200–2500 nm) were obtained on a Varian model Cary 5G (Palo Alto, CA). The refractive indices (η) were measured using a prism-coupling method at 1536.0 nm on polished glass samples. A Metricon model 2010 Prism Coupler instrument (Pennington, NJ), with an index accuracy of 0.001, was used. The emission spectra of Stokes and anti-Stokes photoluminescence were achieved through standard optical setups. The Stokes photoluminescence setup used the 488 nm line of an Ar^+ laser. The infrared emission signal went through a 0.30-m Thermo Jarrel Ash 82497 monochromator (Franklin, MA), and was collected using an EG&G InGaAs photodetector (Wellesly, MA). The upconversion emission spectra were obtained using an 808 and 980 nm AlGaAs diode laser. For these cases, the signal was detected by a photomultiplier tube (Hamamatsu R928, Bridgewater, CA). The measurements of the $^4I_{13/2}$ emission decay curve were carried out with excitation at 980 nm from a Nd:YAG laser-pumped optical parametric oscillator (Continuun Surelite SLII-10, Santa Clara, NJ). The signal was filtered using a monochromator (Thermo Jarrel Ash 82497), collected using an EG&G germanium detector, and processed using a digital oscilloscope (Hewlett Packard 54501A 100 MHZ, Palo Alto, CA). From these curves, the average lifetime values were obtained as those for which the emission intensity drops by a factor 1/e.

III. Results and Discussion

The experimental procedure describes the preparation of homogeneous and bubble-free transparent glasses as reported previously.[3] The $20Na_2O–(5–x–y)Al_2O_3–xEr_2O_3–yYb_2O_3–30Nb_2O_5–15TiO_2–30P_2O_5$ (mol%) glass compositions were chosen for the preparation of planar waveguides because of their tuned properties such as (i) glass stability against devitrification, (ii) optical energy gap, (iii) linear refractive index, and (iv) chemical durability among the glass systems reported previously.[3] These properties were improved as a function of the f_{Nb}/f_{Ti} ratio, where f_{Nb} and f_{Ti} are the atomic molar fractions of Nb and Ti in the glass composition, respectively. As mentioned in the Introduction, in phosphate glasses the Al_2O_3 acts as an ionic cross linker between different chains, inhibiting hydration reactions. For this reason, $Er^{3+}$and Yb^{3+} ions are incorporated into the NAPTN glass systems by aluminum substitutional doping.

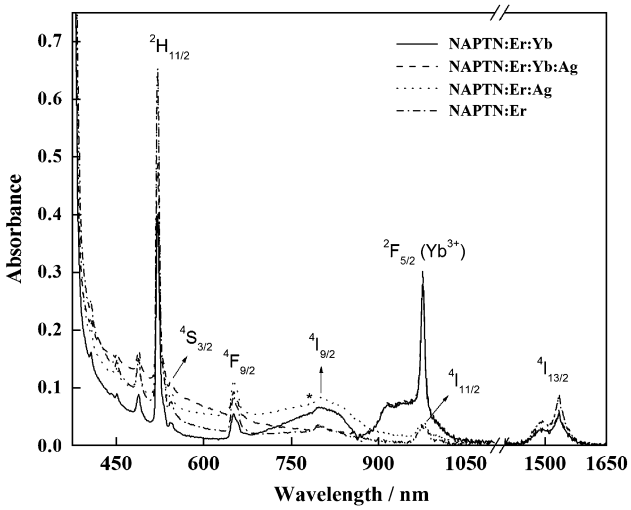

Fig. 1. UV-Vis absorption spectra of as-prepared glasses (NAPTN:Er and NAPTN:Er:Yb) and ion-exchanged glasses (NAPTN:Er:Ag and NAPTN:Er:Yb:Ag). The marked band (*) is an equipment artifact.

The absorption spectra of the rare-earth-codoped samples (Fig. 1) show peaks attributed to erbium and ytterbium trivalent ions, illustrating the higher absorption at 980 nm attributed to the $^2F_{7/2} \rightarrow {}^2F_{5/2}$ transition of Yb^{3+} ion present in Er^{3+}/Yb^{3+}-codoped samples. As shown in Fig. 1, the band attributed to the SPR is not verified, indicating the absence of silver nanoparticles and the good quality of the ion-exchange process. Figure 1 also shows a cut edge absorption assigned to the charge transfer between Nb^{4+} and Nb^{5+}.[2]

As shown in Table II, the samples NAPTN:Ag and NAP TN:Er:Yb:Ag present two guiding modes (TE_0 and TE_1) and the sample NAPTN:Er:Ag is a single-mode (TE_0) planar waveguide at 1536 nm. The refractive index differences between the TE and TM polarizations ($|\eta_{TE}-\eta_{TM}|$) are very small (Table II) for all samples, indicating a negligible birefringence and therefore low stress of the ion-exchanged glasses.

The sample NAPTN:Er:Yb:Ag has the highest variation of the refractive index at 1536 nm ($\Delta\eta = 0.0216$), which has to be decreased in order to obtain single-mode waveguides. This refractive index difference is too high giving more than one guiding mode. Therefore, the ion-exchange parameters have to be improved to adjust the refractive index value and the layer thickness in order to prepare a single-mode waveguide matching silica optical fiber. The thicknesses of the ion-exchanged layers of the samples NAPTN:Ag and NAPTN:Er:Yb:Ag are appropriate to prepare single-mode channel waveguides, matching the silica optical fiber and the thickness of the single-mode NAPTN:Er:Ag sample must be increased to match the core diameter (around 8 μm) of a single-mode silica fiber. Therefore, the results are promising for the preparation of single-mode channel waveguides with weak light confinement.[23]

The emission spectra (Fig. 2) of the erbium- and ytterbium-codoped glass samples present intense and broad bands centered at 1534 nm attributed to the $^4I_{13/2} \rightarrow {}^4I_{15/2}$ transition of

Table II. Refraction Index (η); Number of *Modes* and Thicknesses of the Samples Obtained by M-Lines Spectroscopy at 1536 nm

Sample	η_{TE} (±0.0001)	η_{TM} (±0.0001)	$\lvert\eta_{TE}-\eta_{TM}\rvert$	Δn (TE)†	Modes number	Thickness (μm)
NAPTN	1.8376	1.8377	0.0001	—	—	—
NAPTN:Ag	1.8452	1.8450	0.0002	0.0076	02	7.50
NAPTN:Er	1.8944	1.8941	0.0003	—	—	—
NAPTN:Er:Ag	1.9023	1.9022	0.0001	0.0079	01	2.20
NAPTN:Er:Yb	1.8510	1.8506	0.0004	—	—	—
NAPTN:Er:Yb:Ag	1.8726	1.8726	0.0000	0.0216	02	7.90

†Δn (TE) is equal to the glass refraction index (η_{TE}) before the ion-exchange process minus the glass refraction index (η_{TE}) after the ion-exchange process.

Er^{3+} ions indicating the presence of erbium ions in a noncrystalline environment.

The emission spectra have an average spectral bandwidth of 53 nm, measured at 3 dB from the maximum intensity. It is important to note a higher emission intensity of erbium-doped samples that present silver species in the layer formed on the surface of the glasses after the ion-exchange process (Table II). Based on the UV-Vis spectra (Fig. 1), which shows no evidence of the SPR band characteristic of silver nanoparticles, the intensification of the emission signal verified for silver-containing samples may be attributed to a nonplasmonic energy transfer from silver species to Er^{3+} ions, as proposed by Stohhöfer and Polman.[20] Therefore, the increase of the sample refractive indexes, promoted by thermally assisted ion-exchange processes and the intensification of emission intensity at 1534 nm may indicate the presence of stable Ag^{+} species in the ion-exchanged glass samples and the effectiveness of this process.

The emission decay curves of the erbium $^4I_{13/2}$ metastable state (Fig. 3) were obtained at room temperature upon 980 nm excitation and they are close to an exponential decay curve, indicating a good homogeneity of the chemical environment around the Er^{3+} ions. Yb^{3+} ions inserted into the samples enhance the light absorption at 980 nm. Pumping at this wavelength excites the electrons from the $^2F_{7/2}$ ground state to the $^2F_{5/2}$ manifold. Afterwards, the excited ytterbium(II) ions efficiently transfer their energy to the quasi-resonant $^4I_{11/2}$ erbium(III) state, which in its turn transfers the energy, via nonradiative decay, to the $^4I_{13/2}$ emitting state. Their related average emission lifetime values are around 3 milliseconds, which are lower than those measured in silicate systems[24,25] indicating the existence of a nonradioactive process interaction between erbium(III) ions and multiphonon decay processes that originated from vibrations of the hydroxyl and phosphate groups.

Up-conversion emission measurements show bands attributed to $^2H_{11/2}\rightarrow{}^4I_{15/2}$, $^4S_{3/2}\rightarrow{}^4I_{15/2}$, and $^4F_{9/2}\rightarrow{}^4I_{15/2}$ transitions (Figs. 4 and 5). The efficiency of the up-conversion fluorescence depends on the quantum efficiency of the emitting level as well as the probability of multi-step excitation promoted by absorption of excited states or by energy transfer between adjacent excited ions.

Up-conversion emission experiments of erbium-doped samples by 808 nm excitation are shown in Fig. 4. An intense green luminescence signal corresponding to two bands of the thermally coupled $^2H_{11/2}\rightarrow{}^4I_{15/2}$ (530 nm), $^4S_{3/2}\rightarrow{}^4I_{15/2}$ (547 nm) transitions and also a red luminescence signal at 650 nm attributed to $^4F_{9/2}\rightarrow{}^4I_{15/2}$ transitions are observed.

Up-conversion emission experiments of the erbium–ytterbium-codoped sample by 980 nm excitation are shown in the Fig. 5. This system is one of the most efficient for producing up-conversion by two consecutive processes. In this up-conversion mechanism, an excited Yb^{3+} ion transfers its energy resonantly to an Er^{3+} ion, exciting the latter to the $^4I_{11/2}$ level and the excited Er^{3+} ion reaches the $^4F_{7/2}$ excited level by a second resonant transfer or by excited state absorption. Subsequently, the excited Er^{3+} ions decay nonradiatively from the $^4F_{7/2}$ level to the $^4S_{3/2}$ or $^4F_{9/2}$ levels and return radiatively to the ground state $^4I_{15/2}$, giving green and red emissions, respectively.

To obtain more insight into the up-conversion mechanisms, the dependence of up-conversion intensity was measured as a function of the incident pump power. For any up-conversion mechanism, visible output intensity (I) will be proportional to some power (n) of infrared excitation intensity (P), where n is the number of infrared photon absorbed per visible photon emitted. The insets of Figs. 4 and 5, show a logarithm plot of I versus P for green and red emissions of the ion-exchanged NaPTN:Er:Ag and NaPTN:Er:Yb:Ag samples, respectively. The data were fitted to straight lines, showing a quadratic dependence in both cases indicating that two infrared photons are needed to reach $^4S_{3/2}$ or $^4F_{9/2}$ excited levels. In this case, the excited state absorption can occur from the $^4I_{13/2}$ to the $^2H_{11/2}$ level by the absorption of one more infrared photon. Also, it is im-

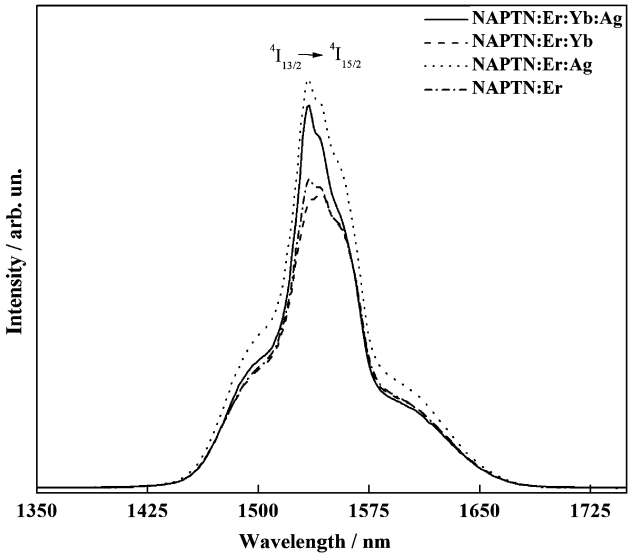

Fig. 2. Photoemission spectra of erbium doped or erbium/ytterbium co-doped silver-free glasses and erbium doped or erbium/ytterbium codoped ion exchanged glasses upon excitation at 488 nm.

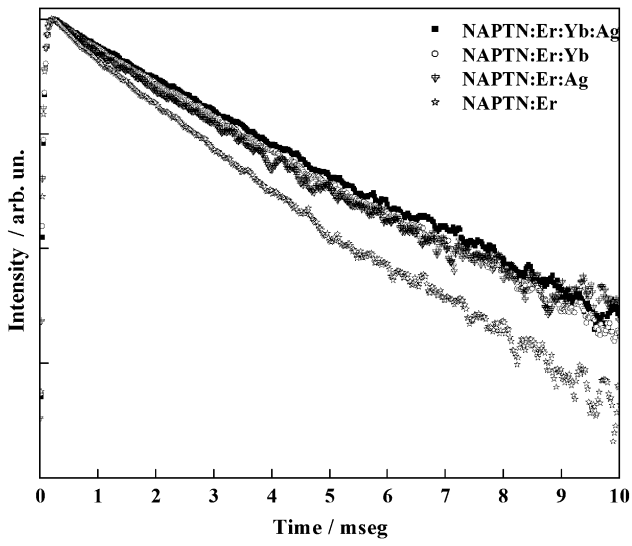

Fig. 3. Luminescence decay curves of the $^4I_{13/2}$ state of the erbium ions upon 980 nm excitation for different samples, as indicated.

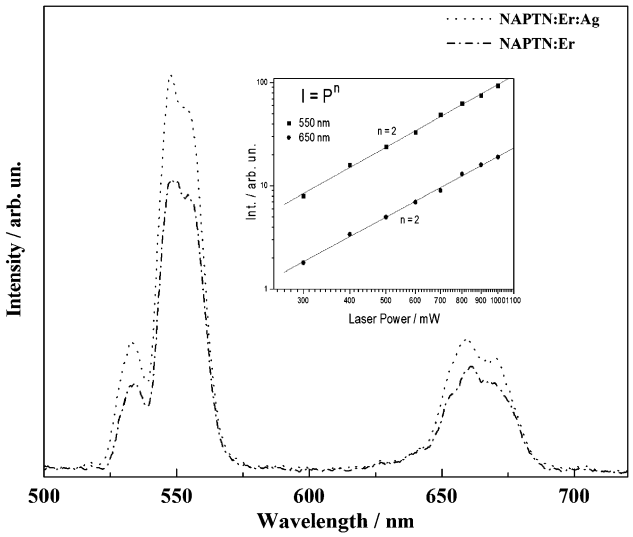

Fig. 4. Up-conversion emission spectra of Er^{3+}-doped samples with CW excitation at 808 nm with several pump powers. The inset shows the dependence of the up-conversion intensity against laser power of the NaPTN:Er:Ag sample.

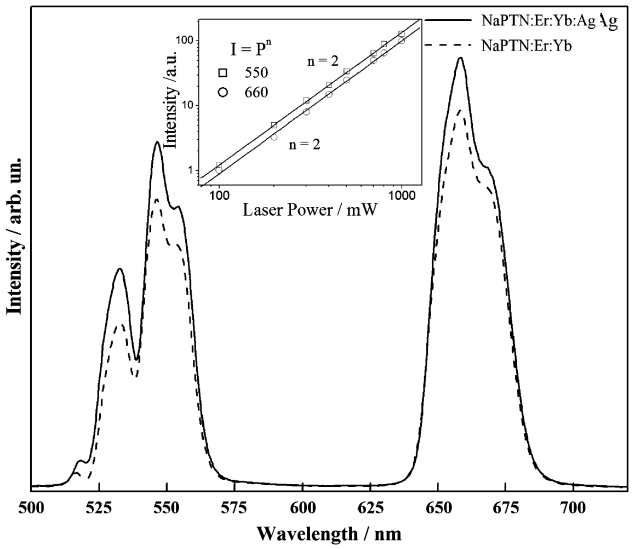

Fig. 5. Up-conversion emission spectra of Er^{3+}/Yb^{3+}-codoped samples with CW excitation at 980 nm with several pump powers. The inset shows the dependence of the up-conversion intensity against laser power of the NaPTN:Er:Yb:Ag sample.

portant to mention a possible second mechanism related to the red up-converted emission. In this mechanism, a second photon promotes the erbium ion to the $^4F_{9/2}$ level by the resonant absorption of the excited state $^4I_{13/2}$. This extra mechanism, to populate $^4F_{9/2}$ without populating $^4S_{3/2}$, results in very strong red luminance, comparable with green emission.

IV. Conclusions

The ion-exchange process has allowed the preparation of single-mode planar waveguides at 1550 nm presenting low birefringence and weak light confinement due to low variation of the refractive index. Therefore, the erbium(III)-doped and erbium(III)–ytterbium(III)-codoped samples show promising optical characteristics and are suitable for ion-exchange processes allowing the preparation of waveguides that can be used for photonic applications. The intensification of the emission signal at 1534 nm verified for silver-containing samples is attributed to a nonplasmonic energy transfer from defects related to silver ions species to erbium(III) ions. The ion-exchanged samples present anti-Stokes emission on the green and red region emission governed by two infrared photon absorption.

Acknowledgments

The authors are grateful to Prof. C. H. Collins (IQ–UNICAMP, Brazil) for English revision. This is a contribution of the National Institute of Science and Technology in Complex Functional Materials (CNPq–MCT/FAPESP).

References

[1]N. Aranha, O. L. Alves, L. C. Barbosa, and C.L Cesar, "The Role of Nb_2O_5 on the Chemical Durability of P_2O_5–Nb_2O_5–PbO–K_2O Glass System"; pp. 282–6 *in Proceedings of XVII International Congress, Glass*, Beijing, 7, 1995.

[2]I. O. Mazali, L. C. Barbosa, and O. L. Alves, "Preparation and Characterization of New Niobophosphate Glasses in the Li_2O–Nb_2O_5–CaO–P_2O_5 System," *J. Mater. Sci.*, **39**, 1987–95 (2004).

[3]Z. Teixeira, I.O Mazali, and O. L. Alves, "Structure, Thermal Behavior, Chemical Durability and Optical Properties of the Na_2O–Al_2O_3–TiO_2–Nb_2O_5–P_2O_5 Glass System," *J. Am. Ceram. Soc.*, **90**, 256–63 (2007).

[4]L. Sirleto, M. G. Donato, G. Messina, S. Santangelo, A. A. Lipovskii, D. K. Tagantsev, S. Pelli, and G. C. Righini, "Raman Gain in Niobium-Phosphate Glasses," *Appl. Phys. Lett.*, **94**, 031105, 3pp (2009).

[5]M. C. Jacqueline, E. R. H. van Eck, G. Mountjoy, R. Anderson, T. Brennan, G. Bushnell-Wye, R. J. Newport, and G. A. Saunders, "An X-Ray Diffraction and ^{31}P MAS NMR Study of Rare-Earth Phosphate Glasses, $(R_2O_3)_x(P_2O_5)_{1-x}$, $x = 0.175$–0.263, R = La, Ce, Pr, Nd, Sm, Eu, Gd, Tb, Dy, Ho, Er," *J. Phys.: Condens. Matter*, **13**, 4105–22 (2001).

[6]L. C. Barbosa, N. Aranha, O. L. Alves, and R. Srivastava, "Ag^+/Na^+ Exchanged Waveguides from Molten Salts in a Chemically Durable Phosphate Glass," *Electron. Lett.*, **32**, 1919–20 (1992).

[7]D. L. Veasey, D. S. Funk, P. M. Peters, N. A. Sanford, G. E. Obarski, N. Fontaine, M. Young, A. P. Peskin, W. C. Liu, S. N. Houde-Walter, and J. S. Hayden, "Yb/Er-Codoped and Yb-Doped Waveguide Lasers in Phosphate Glass," *J. Non-Cryst. Solids*, **263 and 264**, 369–81 (2000).

[8]B. Y. Chen, S. L. Zhao, and L. L. Hu, "Novel Chemically Stable Er^{3+}/Yb^{3+} Codoped Phosphate Glass for Ion-Exchanged Active Waveguide Devices," *Chin. Phys. Lett.*, **20**, 2056–7 (2003).

[9]Y. X. Liu, X. X. Zhang, Y. Li, and Y. Pang, "Properties of Steady-State in Er^{3+}/Yb^{3+} Codoped Phosphate Glass for Optical Waveguide Laser," *Chin. Opt. Lett.*, **5**, 418–21 (2007).

[10]G. W. Shao, G. L. Jin, and Q. Li, "Gain and Noise Figure Characteristics of an Er^{3+}/Yb^{3+} Doped Phosphate Glass Waveguide Amplifier with a Bidirectional Pump Scheme and Double-Pass Configuration," *Opt. Eng.*, **47**, 104201, 7pp (2008).

[11]Y. H. Wang, C. S. Ma, D. L. Li, and D. M. Zhang, "Formulized Analytical Technique for Gain Characteristics of Phosphate Glass Er^{3+}/Yb^{3+} Codoped Waveguide Amplifiers," *Opt. Appl.*, **38**, 329–3 (2008).

[12]H. D. Liu, X. X. Zhang, X. L. Wu, Q. Zhang, and Y. Z. Liu, "Study on Relaxation Oscillation of Er^{3+}/Yb^{3+} Codoped Phosphate Glass Optical Waveguide Laser," *Chin. Sci. Bull.*, **54**, 3653–7 (2009).

[13]Y. H. Wang, C. S. Ma, D. L. Li, and D. M. Zhang, "Effects of Pumped Styles on Power Conversion Efficiency and Gain Characteristics of Phosphate Er^{3+}/Yb^{3+} Codoped Waveguide Amplifiers," *Opt. Laser Technol.*, **41**, 545–9 (2009).

[14]G. Shao, G. Lin, L. Zhan, and Q. Li, "Influence of Multimode-Pump Propagation on the Gain Characteristics of Erbium-Ytterbium Doped Waveguide Amplifier," *Appl. Phys. B*, **97**, 67–71 (2009).

[15]R. D. Shannon and C. T. Prewitt, "Effective Ionic Radii in Oxides and Fluorides," *Acta Cryst. B*, **25**, 925–46 (1969).

[16]G. Jose, G. Sorbello, S. Taccheo, G. Della Valle, E. Cianci, V. Foglietti, and P. Laporta, "Ag^+/Na^+ Ion-Exchange from Dilute Melt: Guidelines for Planar Waveguide Fabrication on a Commercial Phosphate Glass," *Opt. Mater.*, **23**, 559–67 (2003).

[17]S. Yliniemi, Q. Wang, J. Albert, and S. Honkanen, "Studies on Passive and Active Silver-Sodium Ion-Exchanged Glass Waveguides and Devices," *Mater. Sci. Eng. B*, **149**, 152–8 (2008).

[18]F. Ondráček, J. Jágerská, L. Salavcivá, M. Míka, J. Špirková, and J. Čtyroký, "Er–Yb Waveguide Amplifiers in Novel Silicate Glasses," *IEEE J. Quantum Electron.*, **44**, 536–41 (2008).

[19]O. L. Malta, P. A. Santa-Cruz, G. F. de Sá, and F. Auzel, "Fluorescence Enhancement Induced by the Presence of Small Silver Particles in Eu^{3+} Doped Materials," *J. Lumin.*, **33**, 261–72 (1985).

[20]C. Strohhöfer and A. Polman, "Silver as a Sensitizer for Erbium," *Appl. Phys. Lett.*, **81**, 1414–6 (2002).

[21]M. Eichelbaum and K. Rademann, "Plasmonic Enhancement or Energy Transfer? On the Luminescence of Gold-, Silver-, and Lanthanide-Doped Silicate Glasses and Its Potential for Light-Emitting Devices," *Adv. Funct. Mater.*, **19**, 2045–52 (2009).

[22]W. J. Miniscalco, "Erbium-Doped Glasses for Fiber Amplifiers at 1500 nm," *J. Lightwave Technol.*, **9**, 234–50 (1991).

[23]F. A. Sigoli, Y. Messaddeq, and S. J. L. Ribeiro, "Erbium and Ytterbium Co-Doped SiO_2:GeO_2 Planar Waveguide Prepared by the Sol–Gel Route Using an Alternative Precursor," *J. Sol–Gel Sci. Technol.*, **45**, 179–85 (2008).

[24]A. Polman and J. M. Poate, "Ion irradiation in Er-Doped Silica Probed by the Er Luminescence Lifetime at 1.535 μm," *J. Appl. Phys.*, **73**, 1669–74 (1993).

[25]E. Trave, G. Mattei, P. Mazzoldi, G. Pellegrini, C. Scian, C. Maurizio, and G. Battaglin, "Sub-Nanometric Metallic Au Clusters as Efficient Er^{3+} Sensitizers In Silica," *Appl. Phys. Lett.*, **89**, 151121, 3pp (2006). □